# The first Italian BIPV project: Case study and long-term performance analysis

N. Aste, C. Del Pero, F. Leonforte *

Architecture, Built Environment and Construction Engineering A.B.C., Politecnico di Milano, Via Bonardi 9, 20133 Milano, Italy

The estimation of long-term performances of PV systems is a crucial factor for properly assessing the energy and the cost of PV electricity and thus the cost effectiveness of different technologies. This type of prediction is often based on accelerated ageing and tests in indoor condition. However, the combina-tion of different phenomena, such as the mean solar radiation available on the site, the presence of dust, the shadowing or UV radiation over long-outdoor exposure, affect in different ways the real performance of the PV systems.

This paper presents a detailed assessment of the testing campaign on the pilot PV plant at the Politecnico di Milano, which underwent 13 years of continuous operation; such period is particularly rep-resentative because it can be considered as about half of the supposed lifetime cycle of a photovoltaic sys-tem which is usually taken into account for technical–economic evaluations.

The results obtained show that the PV plant analyzed didn't present a significant decrease in long-term performance: the measured PR decay is equal to 0.37%/year. In addition, the visual inspection and IR anal-ysis showed that no PV modules are affected by serious damage. This result is due to a good system design during the preliminary stage, high-quality components and also the back ventilation of the mod-ules, which avoids overheating in the warmer periods of the year.

Finally, an economic analysis was carried out – based on real historical data – which makes the eco-nomic evaluation more reliable.

*Keywords:* Long-term performance, PV degradation, PV reliability, BIPV

## 1. Introduction

The PV market has grown over the past decade at a remarkable rate – even during a difficult economic period – and is on the way to becoming a major source of power generation for the world. After a record growth in 2011, the global PV market stabilized in 2012, and grew again significantly in 2013 (EPIA, 2015).

Considering an application-oriented research, building integrated photovoltaic (BIPV) continues to be emphasized, both for new solutions involving solar cells technology and for new mounting systems and structures for sloped roofs and facades (IEA, 2014).

Since the BIPV offers the possibility to replace part of the traditional building material, with a possible price reduction in comparison to a classic rooftop installation (Campoccia et al., 2014; James et al., 2011), the correct estimation of system-level performances, system reliability and system availability is becoming more important and popular among installers, integrators, investors and owners; with this purpose several tools and models were developed (Aste et al., 2013a,b; Chin et al., 2015; Lo Brano et al., 2014; Zhou et al., 2007). In this sense, the reliable estimation of long-term performances of PV systems is a crucial factor to properly assess the cost of PV electricity, and thus the technologies' affordability. This type of prediction is often based on accelerated ageing and tests carried out according to the IEC 61853. However, the combination of different phenomena, such as the solar radiation available on site, the presence of dust, the shadowing or UV radiation over long outdoor exposure, affect in different ways the real performance of BIPV systems and thus the related economic evaluations (Sharma and Chandel, 2013).

It has to be noted that nowadays, despite the importance of architectural applications for the development and diffusion of PV technology, there are currently no detailed studies on the long-term performance of BIPV systems.

The studies published to date on the performance analysis of PV systems are divided essentially into two categories: those that analyze the modules in laboratory tests (Haillant, 2011; Kajari-Schröder et al., 2012; Muñoz-García et al., 2012; Peng et al., 2012) and those which analyze them in operating conditions (Dolara et al., 2014; Dunlop, 2003; Essah et al., 2014; Granata

*Article history:*
Received 29 December 2015
Received in revised form 22 March 2016
Accepted 9 May 2016
Available online 20 May 2016

* Corresponding author.

*E-mail address:* fabrizio.leonforte@polimi.it (F. Leonforte).


Published Journal Article available at http://dx.doi.org/10.1016/j.solener.2016.05.010

**Nomenclature**

| | | | |
|---|---|---|---|
| $G$ | solar irradiance on the PV modules, W/m$^2$ | $\gamma_m$ | temperature coefficient on power of the PV module, (%/°C) |
| $H$ | annual solar irradiation on the PV modules, Wh/m$^2$ year | $E_{y\text{-}s}$ | energy generated by the PV system during the year, Wh |
| $I_{mp\text{-}m}$ | current of the PV module at the maximum power point, A | $\eta_m$ | nominal efficiency of the PV module |
| $I_{sc\text{-}m}$ | short circuit current of the PV module, A | PR | performance ratio of the PV system |
| $V_{mp\text{-}m}$ | voltage of the PV module at the maximum power point, V | FF | fill factor of the PV module |
| $V_{oc\text{-}m}$ | open circuit voltage of the PV module, V | $K_{PV}$ | overall loss factor related to the PV system |
| $V_{max\text{-}m}$ | maximum system voltage of the PV module, V | $\eta_{inv}$ | inverter conversion efficiency |
| $P_{n\text{-}m}$ | nominal power of the PV module at STC, $W_p$ | MPP | Maximum Power Point |
| $P_{n\text{-}s}$ | nominal power of the PV system at STC, $W_p$ | NPV | Net Present Value |
| $T_e$ | ambient temperature, K | AC | Alternating Current |
| $T_m$ | module temperature, K | DC | Direct Current |
| | | STC | Standard Test Conditions |

et al., 2009; Ishii et al., 2011; Lorenzo et al., 2013; Meyer et al., 2004; Munoz et al., 2011; Polverini et al., 2012; Quintana et al., 2002; Sánchez-Friera et al., 2011).

In addition, papers that analyze PV modules in operating conditions (Dolara et al., 2014; Dunlop, 2003; Granata et al., 2009; Lorenzo et al., 2013; Meyer et al., 2004; Polverini et al., 2012; Quintana et al., 2002; Sánchez-Friera et al., 2011) generally do not give information about the corresponding energy production and plant PR, along with the relative year-by-year variations. Some articles analyzing the PR, instead, give no information on the specific causes that determine its variation (Essah et al., 2014; Ishii et al., 2011).

Being this paper an untapped research step, both aspects (laboratory and field analysis) are dealt with together, in a coordinated manner, focusing specifically on the various technical and non-technical factors affecting performance over time. The results presented can therefore provide a more reliable basis for the design, construction, operation and maintenance of BIPV systems. The aim of this research work is indeed to increase the scientific knowledge on such topic, on the basis of experimental data acquired in the field.

In this sense, an important case-study is represented by the pilot PV plant installed at the Politecnico di Milano University, in so far that it represents the first installation under the national PV Rooftops Programme of the Ministry of Environment in Italy in 2001, and hence the first Italian public funded BIPV plant. The role of such system has a significant importance with respect to the promotion and development of photovoltaic technology, because the plant was carefully designed and installed before the huge development of the PV market in Italy, and also because it is a good example of photovoltaic integration in buildings (see Fig. 1).

This work presents a detailed assessment of the testing campaign on the pilot PV plant, which underwent 13 years of continuous operation; such period can in fact be considered as about half of the supposed lifetime cycle of a photovoltaic system usually considered for technical–economic evaluations.

Therefore, the thorough data provided in this work represent an important benchmark in order to assess the real payback time of any PV application. The information reported is particularly significant, since it is supported by field data and tests carried out in different periods, both in controlled indoor conditions and in outdoor operating conditions.

In detail, the investigation of the degradation of the PV modules, which is the main factor affecting the long-term performance (since the degradation of the inverter can be considered negligible), was carried out by visual inspection, infrared thermography, analysis of actual performance decay over the years and measurement of the $I$–$V$ parameters, as described hereafter.


**Fig. 1.** View of the BIPV system.

Finally, since nowadays the grid parity of the PV technology has been achieved in many Countries, the information about measured and verified long-term performances provided in the paper can contribute to increase the technology attractiveness, by supporting more reliable and accurate energy and economic evaluations.

## 2. Plant description

### 2.1. Architectural and BIPV description

The Politecnico di Milano's 11 kW$_p$ PV plant (latitude 45°27′, longitude 9°11′), installed between 2001 and 2002, represents the first Italian public-funded BIPV intervention, since it is the first implementation carried out under the Photovoltaic Roof Programme, sponsored by the Italian Ministry of Environment (Aste et al., 2007).

The design concept was developed to take advantage, by giving it a new feature, of the slightly sloped roof of Building 11 of the university campus Leonardo da Vinci.

This is an historical building and was designed in the 60s by a team of architects, including Italian "archistars" Piero Portaluppi and Gio Ponti. Due to its peculiar morphology, the roof has favorable characteristics in terms of exposure and solar irradiation, representing an optimal field of application for the installation of a photovoltaic generator. On top of it, in fact, are located 30 skylights with triangular section, arranged in three parallel rows of 10 elements each, which originally guaranteed the natural lighting of the classrooms below. The sheds geometry, as well as their reciprocal inter-distance and the southern exposure on Leonardo da Vinci Park (which guarantees an almost uninterrupted daytime irradiation for the entire year), make these structures perfectly suitable to serve as a support for photovoltaic modules.

A few years after the building construction, because of rainwater infiltration problems, the windows located on the north side of the sheds were obscured and covered with a waterproofing sheath, and lost their original architectural function. Many years later, the PV plant was thus designed to completely cover with its modules the south sides of the sheds. For this purpose, 150 photovoltaic panels have been installed, 73 $W_p$ each, $1220 \times 580$ mm in size, integrating polycrystalline silicon cells and equipped with anodized aluminum frame. The photovoltaic modules are southern oriented, tilted by 65°, positioned in groups of 5 on each skylight and connected together to form 8 strings.

It should be noted that, since the affordability of a PV array is also affected by the self-consumption share of the produced electrical energy (Luthander et al., 2015; Masa-Bote et al., 2014; Widén, 2014), the described PV plant was designed in order to provide an amount of energy which can be instantaneously used to cover part of the building power demand.

During the design phase, special focus was dedicated to the development of the technologies for the mechanical hooking of the modules, which had to be practical and easy to apply, but also ensure the durability and stability of the installation, taking into account the intervention on a quite ancient building, repeatedly subjected to renovations and maintenance works. The interconnection between the photovoltaic panels and the concrete slabs which constitute the south sides of the sheds, in fact, is realized via specially designed clamps, L- and Ω-shaped elements fixed with chemical expansion bolts, sized in such a way as to allow the easy fastening and maintenance of the modules and to leave a ventilated cavity between them and the surfaces behind (Fig. 2). The clamps are made of stainless steel, to avoid the risk of galvanic corrosion of the aluminum frames of the modules. In addition, in order to avoid any direct contact, neoprene sheets were inserted in correspondence of the junction points. The connection adopted provides a 10 cm air–gap between the external waterproof surfaces of the sheds and the PV modules.

It has to be noted that the described BIPV plant, which is primarily demonstrative and has an educational function, was designed taking into consideration not only its productivity and efficiency, but also its appearance and its visibility, since it can be viewed from all over the campus and visited from students and researchers.

Furthermore, from an architectural point of view, it has to be considered that this is a retrofit intervention, on a building not originally designed for solar systems integration. However, the attention to detail, as well as the dimensional analysis and the selection of the mounting technologies have made it possible to harmonize the plant with the existing architecture, avoiding a "fake" effect (see Fig. 3). Also in these aspects lies the value of the project, which has well shown the potential for PV retrofit.

### 2.2. Technical configuration

Each of the 150 mc-Si modules is constituted by a glass-tedlar laminate, which incorporates 36 $12.5 \times 12.5$ cm$^2$ multi-crystalline cells with an efficiency of about 10.6% at Standard Test Conditions (STC). The main features provided by the manufacturer are summarized in Table 1.

The electric configuration consists of 8 strings: six 20-modules strings and two 15-modules strings. Three 3 kW-inverters convert the power from the six 20-modules strings and two 1.1 kW-inverters convert the power from the two 15-modules strings.

**Fig. 3.** Detail of the architectural look.

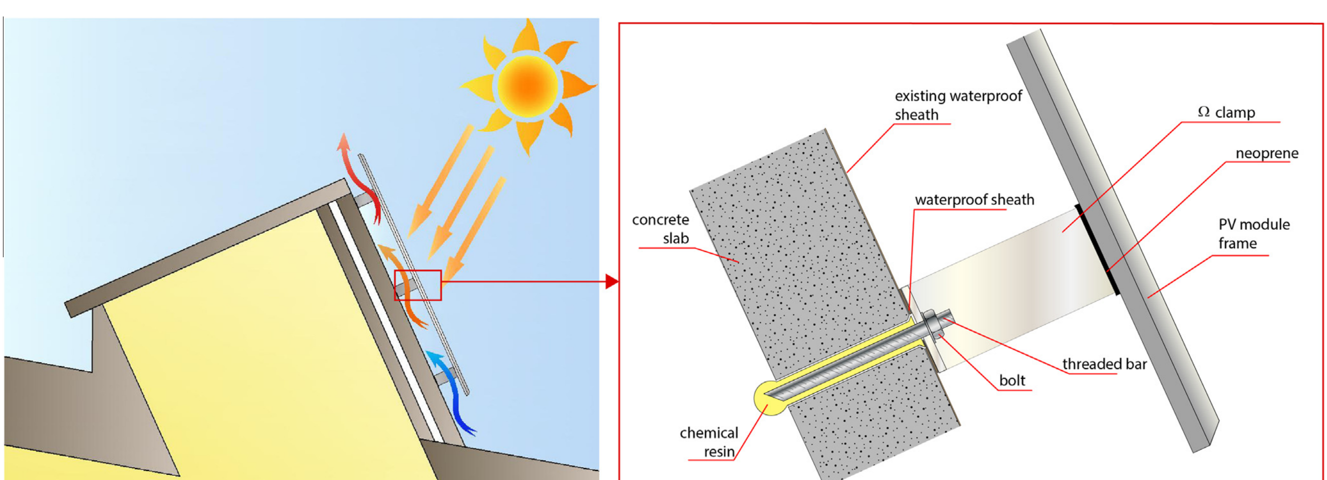


**Fig. 2.** PV modules connection.

**Table 1**
Main electrical parameters of the adopted PV modules provided by the manufacturer.

| | |
|---|---|
| *Electrical characteristics of PV modules* | |
| Nominal power at STC $P_{n\text{-}m}$ (W) | 73 |
| Open circuit voltage $V_{oc\text{-}m}$ (V) | 21.4 |
| Short circuit $I_{sc\text{-}m}$ (A) | 4.6 |
| Voltage at maximum power $V_{mp\text{-}m}$ (V) | 17.0 |
| Current at maximum power $I_{mp\text{-}m}$ (A) | 4.3 |
| Module efficiency $\eta_{\mathrm{m}}$ (%) | 10.3 |
| Fill factor FF (%) | 74.2 |
| Temperature coeff. on power $\gamma_m$ (%/°C) | −0.4 |
| Power tolerance (%) | ±4.0 |
| Maximum system voltage $V_{max\text{-}m}$ (V) | 600 |

The main electrical characteristics of the PV configuration are summarized in the following table (Table 2) and the detailed electric diagram is shown in Fig. 4.

The following table (Table 3) and Fig. 5 show the main characteristics of the inverters and their efficiency curve, respectively.

Although all the inverters are equipped with embedded surge protection devices (SPD), the large extension of the PV array

**Table 2**
Main characteristics of the PV configuration.

| Inverter | AC power (kW) | Strings of PV modules | Total PV modules | String voltage at MPP (V) | String current at MPP (A) |
|---|---|---|---|---|---|
| 1 | 3 | 2 | 40 | 340 | 4.3 |
| 2 | 3 | 2 | 40 | 340 | 4.3 |
| 3 | 3 | 2 | 40 | 340 | 4.3 |
| 4 | 1.1 | 1 | 15 | 255 | 4.3 |
| 5 | 1.1 | 1 | 15 | 255 | 4.3 |

**Table 3**
Main electrical parameters of the adopted Inverter.

| | Inverter 3 kW | Inverter 1.1 kW |
|---|---|---|
| *Electrical characteristics* | | |
| Voltage range MPP tracker (V) | 290–600 | 150–400 |
| Maximum DC rated voltage (V) | 600 | 400 |
| Maximum input current (A) | 11 | 8 |
| Maximum DC power (W) | 3250 | 1230 |
| Maximum ripple DC | 10% | 10% |
| Maximum number of strings | 3 | 2 |
| DC connection | Multicontact | Multicontact |
| Nominal AC voltage (V) | 230 | 230 |
| Maximum AC power (W) | 3000 | 1100 |
| Nominal AC power (W) | 2600 | 1000 |
| Operating temperature range | −25 to +60 °C | −25 to +60 °C |

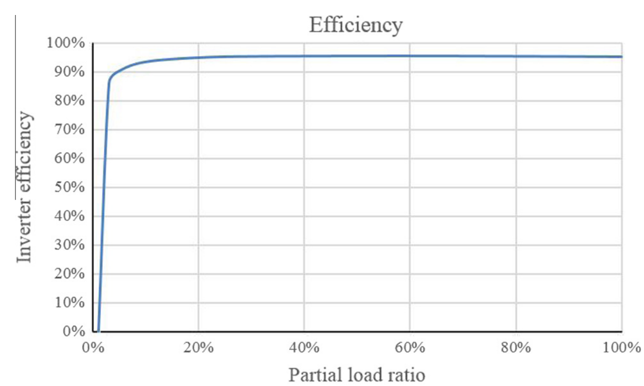


**Fig. 5.** Efficiency curve of inverters.

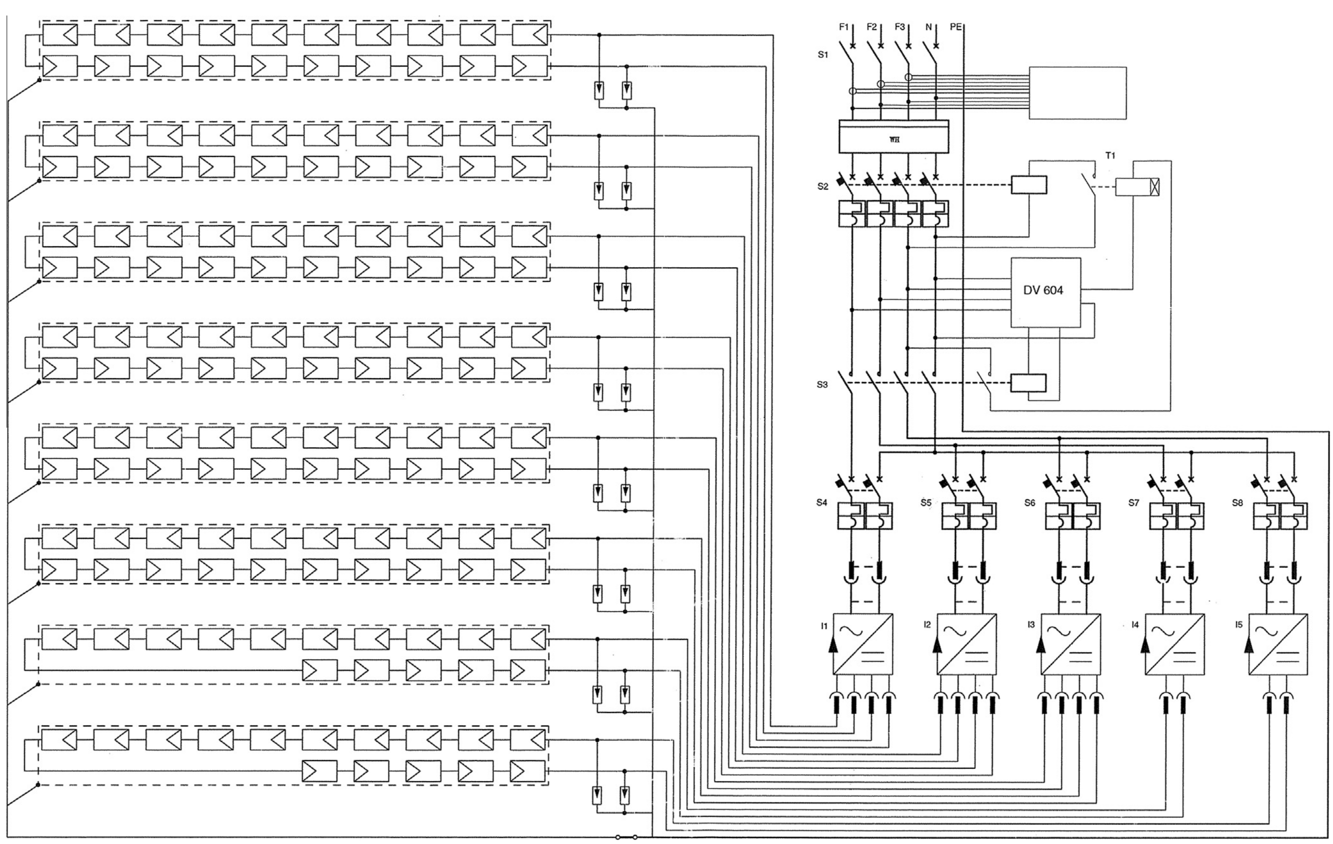


**Fig. 4.** PV system electric diagram.

suggested a reinforcement with further and stronger class II SPD placed near the arrays. Each inverter contains an insulation transformer aimed at electrically separating the DC section from the AC section. In this way the DC section constitutes an IT system, which is a circuit considered safe from electric shocks, even if the open-circuit voltage of the strings should reach 436 V at STC. The DV604 interface device, along with those incorporated in the inverters, provides a good protection against any islanding effect that may be caused by the disconnection of the electric grid.

Since the power supply from the utility to the building is at 20 kV, this voltage value must be internally reduced by means of a 800 kV A transformer. For this reason the PV plant is connected to the 400 V three-phase building grid.

## 3. Performance assessment

### *3.1. Monitoring and data acquisition*

An adequate monitoring of a PV plant is necessary to manage its operation and performance. For this reason, in order to acquire and analyze in detail the performance parameters of the plant, a monitoring system with ambient sensors was installed. This system measures the AC output power and energy from each of the 5 inverters by means of current and voltage sensors, with a final uncertainty on the measured electric power equal to ±1%. The ambient sensors acquire the following quantities:

- Solar irradiance on the module plane $G$ [W/m$^2$], by means of a crystalline silicon reference cell, with an uncertainty of ±5%.
- Ambient temperature $T_e$ [°C] by means of a PT100 sensor with an uncertainty according to A class (IEC, 2008-2).
- PV modules temperature $T_m$ [°C] by means of a PT100 sensor with an uncertainty according to A class (IEC, 2008-2), equal to $\pm(0.15 + 0.0020 \times |T_m|)$.

In order to assess the reliability of the results, an uncertainty analysis was performed on the measurements; in detail, for multiplied or divided independent quantities, the uncertainty on the result can be obtained by calculating and then adding the fractional uncertainties, according to the specifications of the measuring instruments listed above. According to such approach, the final maximum uncertainty on the calculated PR could be considered equal to ±6%. Such value represents the accuracy, which is a quantification of the systematic errors in the measures, in the determination of the PR.

It must be noted that, to contain the uncertainty, a recalibration of the reference cell was carried out every two years.

In addition, it must be specified that the monitoring time step for each parameter is set to 15 min; in fact, longer intervals may interfere with the analysis of the PV plant (Ransome and Funtan, 2005), whereas shorter intervals may overload the monitoring system on long-term analyses.

### *3.2. Overall energy production*

According to the data monitored, it was possible to carry out a detailed energy performance assessment, with the aim of analyzing the actual annual productivity of the plant and of assessing the annual level of performance.

In particular it was observed that, from the installation year until the end of 2014, the plant produced a total amount of approximately 125,000 kW h, with an average production of 9700 kW h/year, which means a production of about 880 kW h/kW$_p$ per year. Analyzing detailed information, the yearly amounts of produced electricity were calculated, as reported in Fig. 6.

It must be noted that, during the working period and more precisely in 2004 and 2008, 2 severe failures of one of the two 1.1 kW inverters occurred. In fact, as is well known, the inverter is one of the most vulnerable components of PV systems (Firth et al., 2010; Zhang et al., 2013). The losses due to such faults were calculated in approximately 300 kW h and 200 kW h, respectively.

### *3.3. Performance data analysis*

In order to identify the performance trend over the 13 operating years, the performance ratio (PR) (Sick and Erge, 2014) for each year was calculated. The PR, which is a crucial parameter for the PV performance evaluation, describes the relationship between the actual and theoretical energy outputs of the PV array. The main equation from the IEC 61724 standard was used to investigate the PR, as reported hereafter:

$$\mathrm{PR} = \frac{E_{y\text{-}s}}{\frac{H}{1000} \times P_{n\text{-}s}}$$

where $E_{y\text{-}s}$ is the energy generated by the PV system during the year [Wh], $H$ is the annual solar irradiation on the PV modules [Wh/m$^2$ -

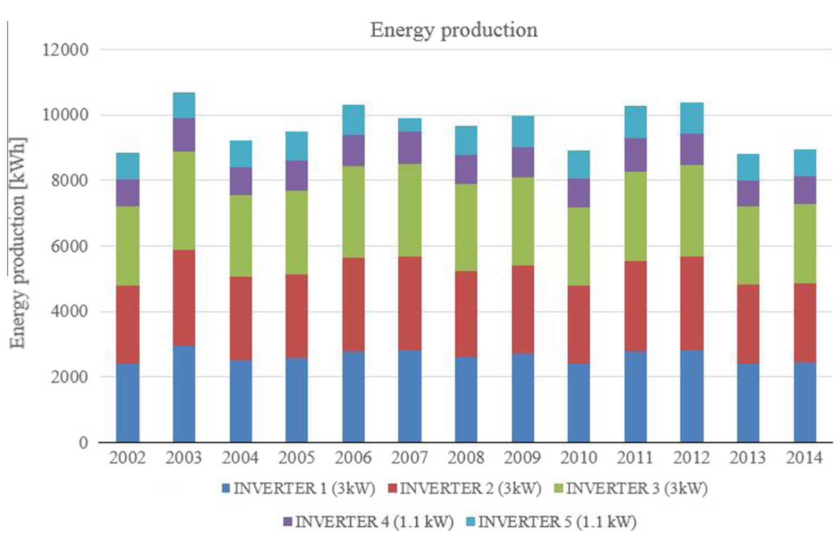


**Fig. 6.** Yearly electricity production.

year] and $P_{n\text{-}s}$ is the nominal power of the system measured at STC [$W_p$].

It is interesting to note that the PR summarizes in a single term the deviation from the standard test conditions (IEC, 1998), caused by the various losses due to the components of the system (such as inverters and cables) and the influence of other external factors (radiation incidence angle, temperature, soiling, etc.). In this sense, PR can be expressed as function of two main factors, as follow:

$$PR = K_{PV} \cdot \eta_{inv}$$

where $K_{PV}$ represents the overall loss factor related to the PV generator due to several parameters, such as: optical reflection reduction factor, quantum efficiency reduction factor, low irradiance reduction factor, module temperature reduction factor, wiring losses reduction factor and soiling reduction factor, and $\eta_{inv}$ represents the average inverter conversion efficiency.

A detailed description of the effects of different factors on the performance of PV plants can be found in literature (IEC, 2008; Jahn et al., 2000; Kymakis et al., 2009; Mondol et al., 2007).

Thanks to the performance assessment described above, it was possible to precisely calculate the behavior of the aforementioned PV system analyzed during its first 13-year working period.

In particular, during the first year of installation, the PR of the BIPV system was calculated as being equal to 70%. Such value can be considered a good result, taking into account the non-optimum tilt angle of the modules and the fact that PV arrays with similar technology installed in Italy in the same period have a PR which varies across a range from 62% to 81% (year 2002), with an average value of 75% (Li Causi et al., 2003).

As shown in Fig. 7, a slight decreasing trend over the years can be identified (about 0.37%/year) and the PR values have a variable fluctuation between +2 and −6 percentage points with respect to the PR calculated in the first year.

Even such amount can be considered a good result if related to the typical degradation rate of mc-Si systems (equal to 0.59%/year) found in literature (Jordan and Kurtz, 2013).

It must be noted that, although a downward trend in annual PR values can be observed, other factors related to seasonal meteorological conditions can be correlated with PR, besides PV module degradation. In particular, in order to take into account the global influence of meteorological conditions, each PR value was correlated with the total number of days without any meteorological event (i.e. sunny days) recorded in each year analyzed, as shown in Fig. 8.

As it can be observed, on average, years with lowers PR (e.g. 2005 and 2010) are also the ones characterized by the greatest number of days with meteorological events (rain, snow, fog), while 2003 is the year with the highest PR and also the maximum recorded number of clear days. This behavior can be related with

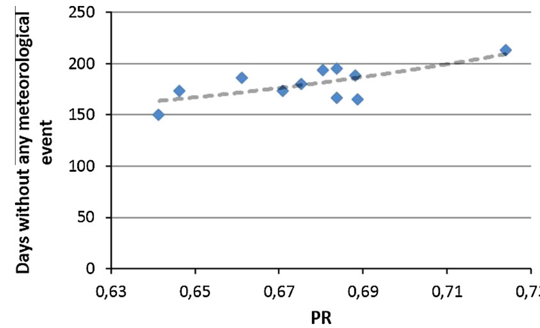


**Fig. 8.** Number of days without any meteorological event and yearly PR.

the decrease in conversion efficiency, which occur in low-irradiance conditions both in the PV modules and in the inverters (Aste et al., 2014; Eikelboom and Jansen, 2000).

In order to better explain the performance trend of the system, the PV modules were analyzed and tested in detail and the results are shown in the following section.

## 4. Module analysis

In this section the main characteristics and the related performance of the PV modules after 13 operating years are analyzed.

PV modules analysis is aimed at identifying all the effects caused by long-term operating conditions, which can directly affect the conversion efficiency of the modules, or simply represent an indication of future technical problems.

In order to better understand the performance trend over the years and the main parameters that affect the energy reduction over the years, a visual inspection and an instrumental inspection, carried out with an IR camera (Flir T640bx) and a *I–V* characterization in STC, were performed after 13 years of outdoor exposure. All the main measurement activities were carried out from the end of 2014 to the end of 2015.

### *4.1. Visual inspection*

The inspections focused on evident visible changes in the modules, such as backsheet yellowing and cracking or delamination of the cells, which can be considered early and first indicators of performance decay, that can lead to more serious problems. The inspection was performed under natural sunlight, to receive a good quality, intense light. Since reflections should be avoided, as they may lead to defective images, the inspection was carried out from

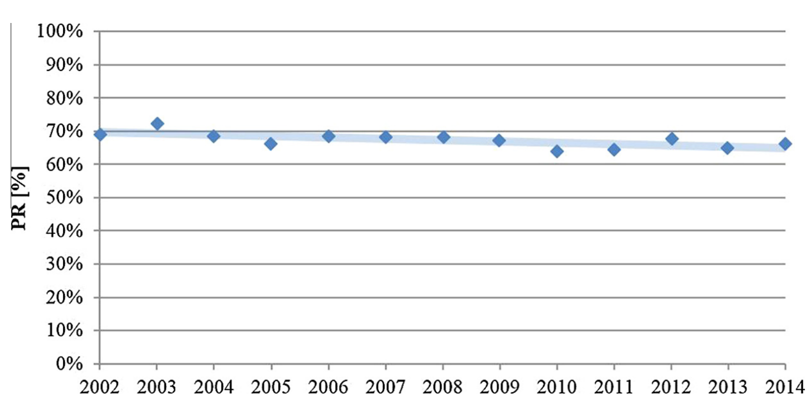


**Fig. 7.** Yearly values of PR.

different angles, to differentiate the layer where the defect could appear and to avoid errors due to reflected images.

In detail, the visual changes and types of defects that were noted during the inspections include:

- slight front side yellowing (100%, 150 modules);
- delamination and presence of bubbles on the cell (12%, 18 modules);
- delamination along busbars (52%, 79 modules);
- cracking of the cell (10%, 15 modules);
- misaligned soldering (1%, 2 modules).

As it can be noted, all modules show a front yellowing. It consists of a degradation of the EVA layer located between the glass and the cells. It is a color change in the material from transparent to yellow and in some cases from yellow to brown (Dechthummarong et al., 2010; Ndiaye et al., 2013). It causes a change in the transmittance of the solar radiation reaching the solar cells, and thus a decrease in the power generated. Generally, according to some experimental work (Realini, 2003), the correlation between electrical characteristics and encapsulant discoloration showed that completely yellowed modules present a decrease in $I_{sc\text{-}m}$ up to 13% with respect to the module with no change in color. It should be noted that numerous modules are also characterized by backsheet yellowing, which typically occurs when encapsulants are exposed for prolonged time to UV rays.

Together with the front and back yellowing, cell delamination represents the second largest visual defect observed. It consists in the loss of adherence between the different layers of the PV module and the subsequent detachment of parts of these layers, such as the cells and the front glass (Munoz et al., 2011). Delamination was observed particularly in the cells above the Junction Box (Fig. 9A) or along the busbars (Fig. 9B). Due to delamination, a reduction in the radiation that reaches the solar cell and hot spot phenomena may occur. However, delamination doesn't necessarily imply a performance drop, since it depends on the total area affected by the defect (Realini, 2003).

An example of cell micro-cracking, which is shown as a discoloration of the fine conductor lines overlaying a crack or micro-crack in the cell, resulting from the interaction of EVA encapsulant additives and silver, is shown in Fig. 9C.

Since the cracks may remove portions of the cell from the electrical contact, the power output of the module can decrease consequently (Munoz et al., 2011).

Finally, the misaligned soldering of the busbars (Fig. 9D), which may lead to an increase in current resistance along the cells, and

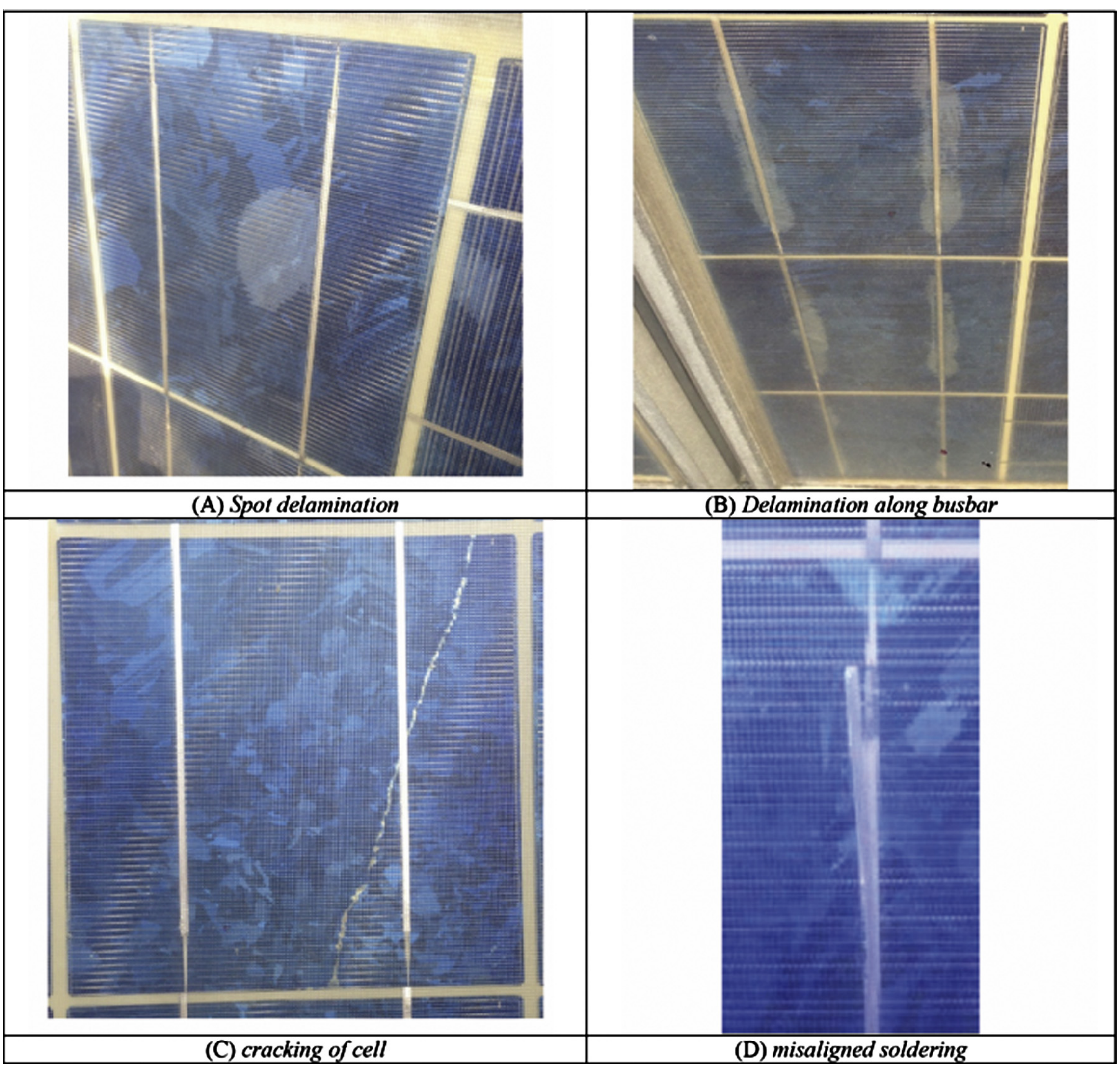


**Fig. 9.** Main visible changes detected.

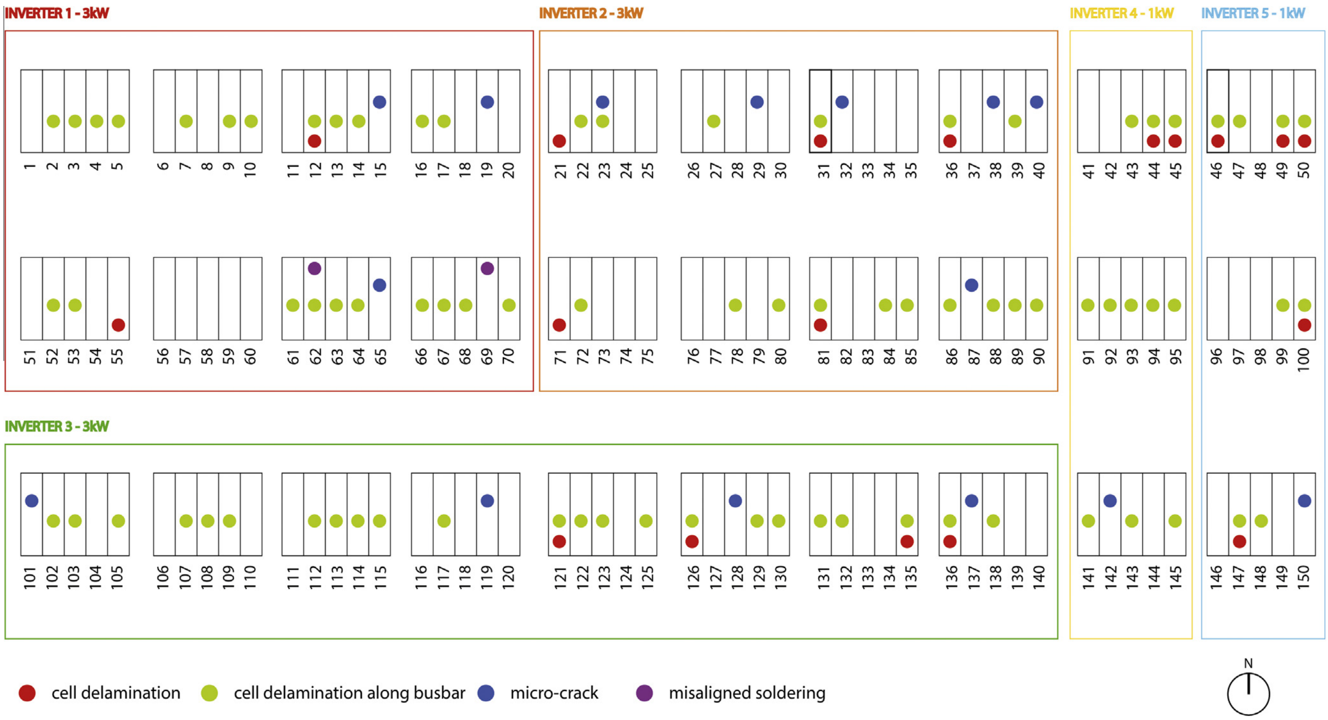


**Fig. 10.** Position of modules with defects.

thus to an increase in cell temperature, was detected in two modules (García et al., 2013). However, it must be specified that misaligned soldering is not an effect of ageing, but was included in the analysis as a defect of the modules.

Not all the inspected modules had some level of visible defects. However, it should be noted that the overall state of the PV module appears good and the chemical degradation of the material seems to be low.

In order to clarify the relation between the distribution of the defects on the PV array and the productivity output from each inverter, the results of the visual inspection are reported in Fig. 10, according to the real configuration of the system. More in detail, the main defects are identified in the scheme with colored[1] bullet.

By analyzing the spatial distribution of the defects listed above, it is possible to assert that there isn't any evident correlation between the position of the modules and the presence of defects.

### 4.2. IR inspection

In order to identify possible module failures or overheating phenomena due to the aforementioned cell defects, an IR analysis was carried out with the Flir T640bx.

Using thermal imaging cameras, the entire array was examined, checking the possibility of hot spots. The images were taken from the front side, since the modules are building integrated components and it was not feasible to carry out a thermal analysis on the back side in operating conditions. Special care was taken in order not to include sun reflection during the IR evaluations. The emissivity of the module was set to 0.85, which is a typical value for the glass, while the sky temperature was evaluated as equal to 10 °C.

[1] For interpretation of color in Fig. 10, the reader is referred to the web version of this article.

As expected, the cells above the junction box were approximately 3–10 °C hotter than the rest of the PV module. As a consequence, in such points the PV cells have a different temperature and, thus, a different electrical performance.

In addition, the modules located in the external part of the sheds are cooler (by almost 3 °C) than the panels located in the middle part of the structure. This difference is due to the influence of ventilation on the PV modules, which is more effective in the edge of each shed.

In order to analyze the electrical performance of the modules subjected to different temperatures along the strings, with regard to the uniform temperature distribution, two calculations were carried out on the energy output of inverter 1, according to the module features. The first was performed considering the real mean temperature distribution of the modules (shown in Fig. 11) and the second considering that all the PV modules were at the same mean temperature of the module located in the middle part, equal to 43 °C.

The results obtained are summarized in the following table.

As shown in Table 4, the difference in terms of electrical power between the two temperature distributions analyzed is almost negligible.

Finally, it is important to note that, in a few points, some slight hot spots were also identified, as shown in Fig. 12 (e.g. "SP1" point). However, despite the higher temperature detected with the IR analysis on the cells surface, with an increase of up to 10 °C, no defects or localized deterioration was observed on the front side upon a visual inspection, as a consequence of such overheating. In fact, according to literature (Moretón et al., 2014), in the presence of a temperature increase of a certain PV cell in relation of the other cells of the same module lower than 10 °C, no significant defects of the module (e.g. deep micro-cracks, significant defective soldering, potential induced degradation, etc.) have to be considered. For such reasons, it is not possible to ascertain if this overheating is due to an anomalous degradation of the PV cell concerned, or to a manufacturing defect already present at the beginning of the operating period.

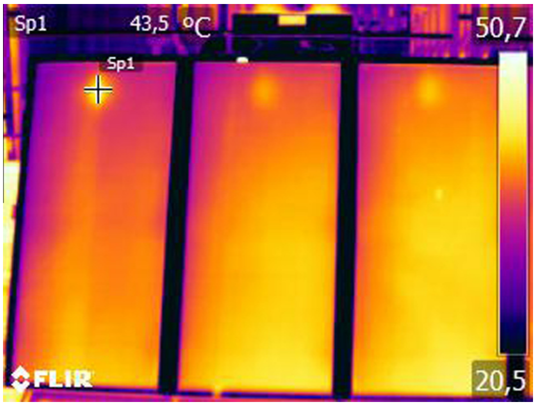


**Fig. 11.** IR image of modules 6, 7 and 8.

**Table 4**
Main electrical performance parameters of the string (Inverter 1).

| | Real distribution | Hypothetical distribution |
|---|---|---|
| String current at MPP (A) | 8.645 | 8.654 |
| String voltage at MPP (V) | 319.95 | 318.52 |
| String power at MPP (W) | 2766.02 | 2756.52 |

*4.3. (Flash test) IV characterization*

After 13 years of outdoor exposure, 4 modules (module 31, 138, 150, 140) characterized respectively by spot delamination, delamination along the busbar, cell cracking and hot spot, and one module without any visual defect (module 51), were removed from the array in 2015, in order to test the *I–V* curve in standard test conditions, following the procedure defined in IEC 60904. The test was carried out at the EURAC laboratory, using a PASAN testing chamber, with a 2.8% accuracy and a 0.2% repeatability.

The main results of the testing activity carried out are summarized in the following table. It must be noted that the values are referred to clean PV modules.

Unfortunately it is not possible to clearly assess the deviation compared to the original state of the modules analyzed, since the *I–V* characterization at the installation of the PV array is missing and only technical datasheets are available.

However, a comparison between the reference values reported in the datasheets (considering a tolerance of ±4% on the nominal power) and the *I–V* characterization after 13 years can be done.

In the case where the initial nominal power of the modules was 73 W, the 13 years decay level can vary between 3.6% and 13.8%, according to the measurements on module 31 and 140 respectively, while – considering the minimum power guaranteed by manufacture – the difference varies from −0.41% (which means than no degradation occurred on the module 31 tested) to 10.2% for the module with the slight hot spot.

It is important to note that the modules characterized by delamination (31 and 138) show a performance reduction in agreement with the result obtained from the long-term performance analysis described in Section 3.3 (close to 0.37%/year). On the contrary, cracking defects and hot spots have a greater influence on the PV performance of the module, as shown in Table 5.

Finally, since the module characterized by the slight hot spot shows the greatest deviation in terms of power versus the value stated by the manufacturer, more in-depth analyses have been carried out on such component. More in detail, each string of the module was tested separately in STC. According to the results listed in Table 6, the string of the module which contains the cell with the slight hot spot shown in Fig. 12 (left string) affects the performance of the entire module with a power output in STC 16% lower than that of the other string (right string).

The detailed analysis on the module affected by the slight hot spot indicates that, in accordance with the literature (Moretón et al., 2014), the phenomenon observed is not particularly serious, since the cell overheating is lower than 10 °C and the power loss of the affected string in STC is limited; thus, it is not a symptom of severe problems in the PV cell, such as deep micro-cracks, but can be mainly related to a manufacturing defect of the cell. However, the performance of such module will be carefully monitored in the future, to assess any further problems.

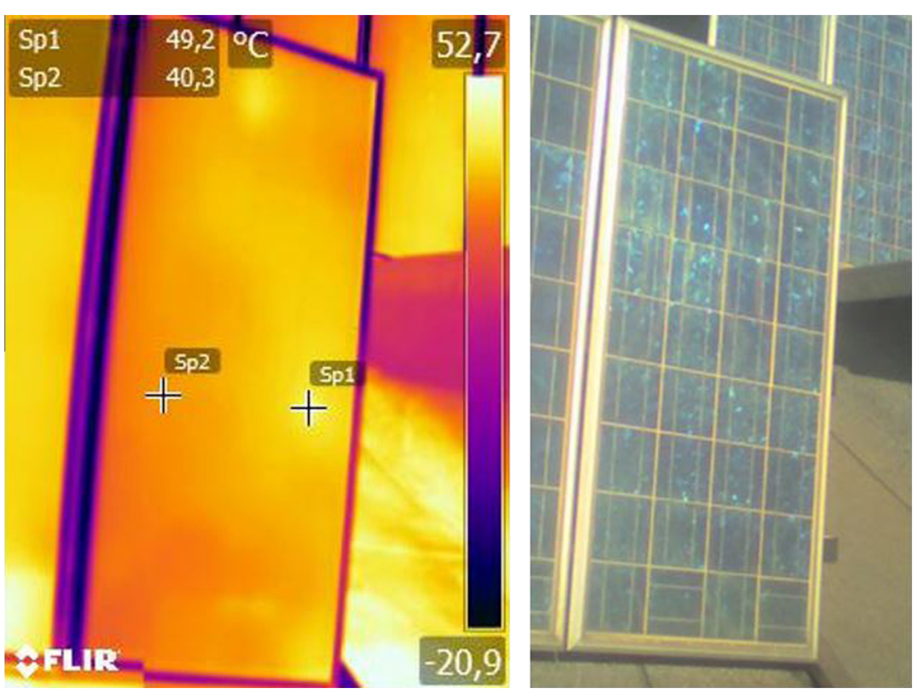


**Fig. 12.** PV module 140.

**Table 5**
Main results of the testing activity.

| | Module 31 (spot delamination) | Module 138 (delamination along busbars) | Module 150 (cell cracking) | Module 140 (hot spot) | Module 51 (no visual defects) | Reference values from datasheet |
|---|---|---|---|---|---|---|
| Nominal power at STC $P_{n\text{-}m}$ (W) | 70.37 | 67.00 | 65.73 | 62.87 | 67.73 | 73 (±4%) |
| Open circuit voltage $V_{oc\text{-}m}$ (V) | 21.51 | 21.46 | 21.43 | 21.51 | 21.35 | 21.4 |
| Short circuit current $I_{sc\text{-}m}$ (A) | 4.47 | 4.34 | 4.21 | 4.29 | 4.21 | 4.60 |
| Fill factor FF (%) | 73.16 | 71.99 | 72.08 | 68.16 | 75.35 | 74.20 |
| Power reduction respect to declared performance (73 W) (%) | 3.6 | 8.2 | 10.4 | 13.8 | 7.2 | – |
| Power reduction respect to minimum guaranteed performance (70.08 W) (%) | −0.41 | 4.6 | 7.10 | 10.2 | 3.4 | – |

**Table 6**
Results of the detailed flash test carried out on the 2 strings of module 140.

| | Module 140 | (Left string) | (Right string) |
|---|---|---|---|
| Nominal power at STC $P_{n\text{-}m}$ (W) | 62.87 | 28.75 | 33.31 |
| Open circuit voltage $V_{oc\text{-}m}$ (V) | 21.51 | 10.69 | 10.72 |
| Short circuit current $I_{sc\text{-}m}$ (A) | 4.29 | 4.26 | 4.32 |
| Fill factor FF (%) | 68.16 | 63.17 | 71.93 |

### *4.4. Soiling analysis*

Flash tests at STC were carried out both with PV modules in their state of fouling and after a deep cleaning of the glazed surfaces, in order to assess the effect on energy performance of the dust layer resulting from long-term outdoor exposition without cleaning. In detail, analyzing the maximum power before and after the cleaning, a decreasing from 0.2% to 2.0% was recorded. It must be specified that 0.2% is the repeatability of the measure carried out with the testing chamber. The data was summarized in Table 7.

**Table 7**
PV performance comparison before and after cleaning.

| | Measured power at STC (W) | | |
|---|---|---|---|
| | Clean | Dirty | % reduction |
| Module 31 | 70.37 | 68.97 | 2.0 |
| Module 138 | 67.00 | 66.86 | 0.2 |
| Module 150 | 65.73 | 65.43 | 1.8 |
| Module 140 | 62.87 | 61.92 | 1.5 |
| Module 51 | 67.73 | 67.28 | 0.7 |

The difference in the influence of soiling among the tested PV modules is small (1.8%) and can be related to the different position of the modules in the plant; in fact, PV modules are subjected to several types of soiling, such as dust, large and small particulate, bird droppings etc, which can behave in different ways, according to the specific location in which the PV module is installed.

Moreover, in order to better understand the influence of dust on the PV performance in real operating conditions, an experimental analysis on PV strings connected to two different inverters, with comparable characteristics and energy trends, was provided. In fact, the PV sections connected to such inverters typically recorded very similar energy productions over the years analyzed. More in detail, the daily energy production of inverters No. 1 and No. 3 was compared during some sample days, before and after the cleaning of all the PV modules connected to inverter No. 3.

Fig. 13 shows the daily energy outputs for 5 days (from 24/09/2014 to 28/09/2014). Comparing the results obtained before and after the cleaning of the modules connected to inverter No. 3, an increase between 2.7% and 3.3% was registered. The reported values are in agreement with the flash test results.

The results obtained are coherent with those of a similar research (Appels et al., 2013), where it is demonstrated that the impact of soiling typically reaches its saturation after 30–50 days of exposure and, for modules with high tilt angle, as in the case study considered, the stabilized loss due to soiling is on average less than 3%. In fact, rain has a little cleaning effect on smaller dust particles, but on bigger particles the cleaning effect is clearly visible.

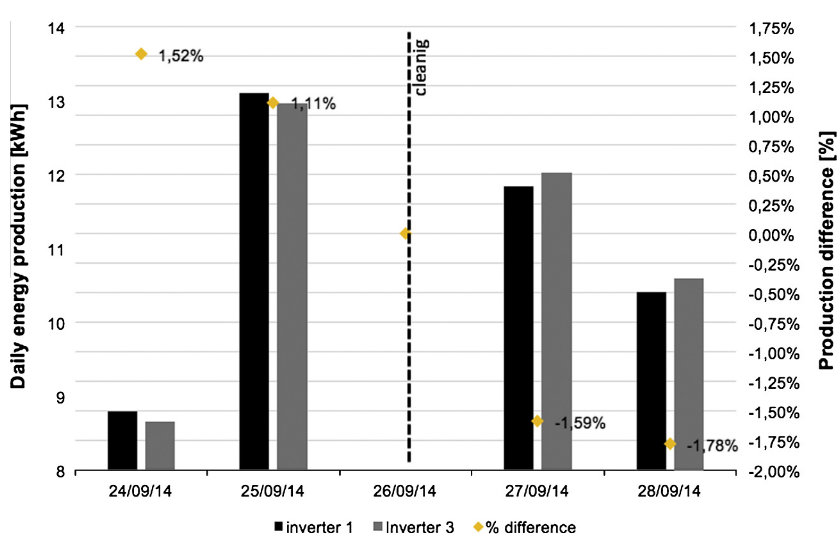


**Fig. 13.** Daily energy outputs of inverter 1 and 3 during 5 days in a row.

### 4.5. Back side ventilation

As already said, each module of the array plant is installed in order to provide a 10 cm air–gap between the external shed surfaces and the PV module. This solution allows to maintain the temperature of the modules lower than a standard BIPV, that is generally attached to an insulation material. The increase in temperature of the modules, in fact, causes the reduction of the band gap of the PV cells (Kalogirou, 2013). This leads to a higher decrease in $V_{OC}$ than the increase in $I_{SC}$, which means that the overall power output of the PV modules decreases with the increase in its operating temperature.

In this sense, in order to evaluate the benefit due to the convective air flow on the back sheet of the PV module, a 10 cm thick insulation layer (thermal conductivity 0.035 W/m K) was placed between the existing shed and module 32. The surface temperature of the insulated module was analyzed with an IR camera and compared with the adjacent, non-insulated PV module. The IR acquisition was carried out during a sunny day, with an ambient temperature of 18.7 °C and a wind speed equal to 3 m/s, recorded at the moment of the analysis.

As shown in Fig. 14, the maximum surface temperature of the insulated module is about 57 °C, while the non-insulated one is about 40 °C, which leads to a difference in power output of about 11%. In terms of overall power production, the insulated module causes a reduction of about 0.31% in the total power output of inverter 2.

## 5. Economic analysis

Economic assessments of grid-connected PV plants are usually based on the expected electricity production obtained through energy simulation (Reinders et al., 1999), average O&M costs over the system operating life, typically considered as a percentage of the installation cost (Orioli and Di Gangi, 2014), and electricity cost trends. Unfortunately, sometimes such estimations turn out to be unreliable, because of inaccurate system losses evaluation, wrong plant availability forecast and under-overestimated costs and benefits. Consequently, a certain risk must be taken in account, unless real and affordable data on long-term performances are known.

In this work, the economic analysis is based on real historical data, referred to half of the operating life of the system, which makes the economic evaluation more reliable. In particular, detailed costs paid in 2001 for the realization of the PV system (before VAT) are reported as follows:


**Fig. 14.** IR image of module 32.

- solar modules: 53,091€;
- inverters: 7798€;
- switchboards, wiring: 3800€;
- mounting system: 6296€;
- installation: 8495€;
- design and project management: 7800€.

As can be noted, total cost of the plant is equal to 7792 €/kW$_p$
The public grant covered about 75% of the total cost of the plant, with an amount equal to 66,600€ and hence a remaining cost equal to 20,700€. As for the components and the planning/design costs, in the calculation only the fraction related to the PV plant was considered, excluding the data acquisition system and the remote display. The remaining total cost due to such components was equal to 24,600€.

Actual O&M costs recorded during the operating period are instead the following:

- repairing of a 1.1 kW inverter: covered by the manufacture warranty (year 2004);
- repairing of a 1.1 kW inverter: 600€ (year 2008);
- repairing of the monitoring system: 1000€ (year 2009);
- deep cleaning of the PV modules and general check: 400€ (year 2010).

The above-listed operation and maintenance costs, referred only to the PV plant (thus excluding those related to the monitoring system), are approximately equal to 1000€, that is 1.1% of the total installation cost, and is less than 0.05%/year.

In addition, with the aim to calculate the value of the electrical energy substituted by the PV plant, the real electricity price paid by the University during the operating life of the system was recorded and reported in the following table (Table 8).

Taking into account the real market prices recorded from 2002 to 2014 and the expected electricity cost trend for the next years with the same growth rate recorded in such period, the average value for the Politecnico from 2002 to 2027 (theoretical end-of-life of the plant) is expected to be equal to approximately 0.21 €/kW h. The overall market value of the produced electricity during the 25 years operating life can consequently be calculated as equal to 240,000 kW h $\times$ 0.21 €/kW h = 50,400€.

On the basis of these considerations, the discounted cash flow can be easily calculated, demonstrating that the investment payback time, equal to 12 years, has been recently reached (Aste et al., 2013a,b).

Moreover, once the actual energy production, the yearly degradation rate and the O&M costs are known, it's worth it to assess the economic performance of the same PV system, assuming it was realized in the year 2014, thus with the current costs of technology and electricity. Such analysis represents a reliable and trustworthy forecast of the future economic yield of well-designed and well-realized BIPV systems, based on the real half-life operating data of the monitored plant.

**Table 8**
Actual electricity costs paid by the University from 2002 to 2014 (before VAT).

| Year | Cost (€/kW h) | Year | Cost (€/kW h) |
|---|---|---|---|
| 2002 | 0.105 | 2009 | 0.149 |
| 2003 | 0.109 | 2010 | 0.158 |
| 2004 | 0.114 | 2011 | 0.165 |
| 2005 | 0.121 | 2012 | 0.173 |
| 2006 | 0.129 | 2013 | 0.179 |
| 2007 | 0.137 | 2014 | 0.193 |
| 2008 | 0.145 | | |

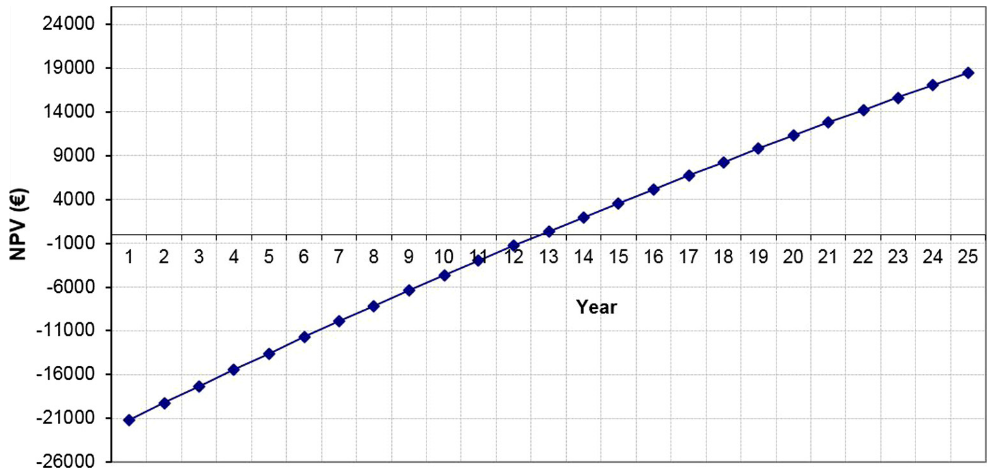


**Fig. 15.** NPV and payback time calculation considering the current system realization cost and actual energy performances/O&M costs.

In this sense, considering the current PV technology market prices in Italy, this realization cost of the plant analyzed (before VAT) was estimated according to the following assumptions:

- solar modules: 7260€ (0.66€/$W_p$) (PvXchange, 2015);
- inverter: 1800€ (1 three-phase multistring inverter with 2 MPPTs) (IHS, 2013);
- switchboards, wiring: 2500€ (diodes and DC-parallel boards can be avoided);
- mounting system: 2500€ (few custom solutions are needed);
- installation: 6000€ (less labor needed, thanks to the simpler configuration);
- design and project management: 3000€ (lower technical complexity).

According to the aforementioned estimate, the total cost of the same system realized at the end of 2014 should be equal to approximately 23,060€, corresponding to roughly 2096 €/$kW_p$, It means that, thanks to incentive polices and consequent market development, a reduction in the market cost of PV systems close 70% has been achieved from 2002 to 2014.

The discounted cash-flow over 25 years was thus re-calculated with the above realization costs, considering for the first 13 years the actual energy performance and O&M costs recorded and assuming for the second half-life period the same trends (performance degradation equal to 0.4%/year and O&M expenses equal to roughly 90€/year). Consequently, the net present value (NPV) and the economic payback time of the system were estimated, as shown in Fig. 15. An interest rate equal to 3% was assumed and all the energy produced was presumed to be instantaneously used to directly cover the building's electricity demand, as in the real operating conditions of the analyzed system.

The results obtained show that the system analyzed, if realized at the end of 2014, is able to maintain the same payback time period also without any subsidy. The NPV is indeed equal to approximately 19,300€ and the payback is reached before the end of the twelfth operating year.

## 6. Conclusions

The pilot PV system of the Politecnico di Milano, which is the first installation under the Italian PV Rooftop Programme, was presented and evaluated, since it represents a reference for the design and realization of photovoltaic plants in urban context.

In fact, during the 13 years of operation, it was observed that the plant analyzed didn't show a significant decrease in performance: the PR decay measured is equal to 0.37%/year, which is less than the usually considered degradation in mc-Si system (equal to approximately 0.6%/year). Moreover, visual inspection and IR analysis showed that no PV module is affected by serious damage. This result is due to a good system design during the preliminary stage, high-quality components and also back ventilation of the modules, which avoids overheating in the warmer periods of the year.

Compared to the current PV market, the results confirm that PV systems might work effectively during the 25 years standard operating life considered for technical–economic evaluations, ensuring good energy and economic performances, also without any subsidy.

Finally, the collected data can act as a useful database to understand in detail the performance of BIPV plants under real condition over time.

## References


Appels, R., Lefevre, B., Herteleer, B., Goverde, H., Beerten, A., Paesen, Poortmans, J., 2013. Effect of soiling on photovoltaic modules. Sol. Energy 96, 283–291. http://dx.doi.org/10.1016/j.solener.2013.07.017.

Aste, N., Adhikari, R.S., Tagliabue, L.C., 2007. Evaluation of energy policies for promotion and dissemination of photovoltaic technology in Italy. Prog. Photovoltaics Res. Appl. 15, 449–460. http://dx.doi.org/10.1002/pip.751.

Aste, N., Del Pero, C., Leonforte, F., 2014. PV technologies performance comparison in temperate climates. Sol. Energy 109, 1–10. http://dx.doi.org/10.1016/j.solener.2014.08.015.

Aste, N., Del Pero, C., Leonforte, F., 2013a. The first installation under the Italian PV Rooftop Programme: a performance analysis referred to 11 years of operation. In: 2013 International Conference on Clean Electrical Power (ICCEP). IEEE, pp. 628–633. http://dx.doi.org/10.1109/ICCEP.2013.6586951.

Aste, N., Del Pero, C., Leonforte, F., Manfren, M., 2013b. A simplified model for the estimation of energy production of PV systems. Energy 59, 503–512. http://dx.doi.org/10.1016/j.energy.2013.07.004.

Campoccia, A., Dusonchet, L., Telaretti, E., Zizzo, G., 2014. An analysis of feed'in tariffs for solar PV in six representative countries of the European Union. Sol. Energy 107, 530–542. http://dx.doi.org/10.1016/j.solener.2014.05.047.

Chin, V.J., Salam, Z., Ishaque, K., 2015. Cell modelling and model parameters estimation techniques for photovoltaic simulator application: a review. Appl. Energy 154, 500–519. http://dx.doi.org/10.1016/j.apenergy.2015.05.035.

Dechthummarong, C., Wiengmoon, B., Chenvidhya, D., Jivacate, C., Kirtikara, K., 2010. Physical deterioration of encapsulation and electrical insulation properties of PV modules after long-term operation in Thailand. Sol. Energy Mater. Sol. Cells 94, 1437–1440. http://dx.doi.org/10.1016/j.solmat.2010.03.038.

Dolara, A., Leva, S., Manzolini, G., Ogliari, E., 2014. Investigation on performance decay on photovoltaic modules: snail trails and cell microcracks. IEEE J. Photovoltaics 4, 1204–1211. http://dx.doi.org/10.1109/JPHOTOV.2014.2330495.

Dunlop, E.D., 2003. Lifetime performance of crystalline silicon pv modules. Photovoltaic Energy Convers., 2927–2930

Eikelboom, J., Jansen, M., 2000. Characterisation of PV modules of new generations, ECN-C-00-067 Results of Tests and Simulations.

EPIA, 2015. Global market outlook for solar power 2015–2019 [WWW Document]. 2015 <http://resources.solarbusinesshub.com/images/reports/104.pdf>.

Essah, E.a., Rodriguez Arguelles, A., Glover, N., 2014. Assessing the performance of a building integrated BP c-Si PV system. Renew. Energy 73, 4–13. http://dx.doi.org/10.1016/j.renene.2014.04.002.

Firth, S.K., Lomas, K.J., Rees, S.J., 2010. A simple model of PV system performance and its use in fault detection. Sol. Energy 84, 624–635. http://dx.doi.org/10.1016/j.solener.2009.08.004.

García, M., Marroyo, L., Lorenzo, E., Marcos, J., Pérez, M., 2013. Observed degradation in photovoltaic plants affected by hot-spots. Prog. Photovoltaics Res. Appl. 22, 1292–1301. http://dx.doi.org/10.1002/pip.2393.

Granata, J.E., Boyson, W.E., Kratochvil, J.A., Quintana, M.A., 2009. Long-term performance and reliability assessment of 8 PV arrays at Sandia National Laboratories. In: Photovolt. Spec. Conf. (PVSC), 2009 34th IEEE, pp. 1486–1491. http://dx.doi.org/10.1109/PVSC.2009.5411336.

Haillant, O., 2011. Accelerated weathering testing principles to estimate the service life of organic PV modules. Sol. Energy Mater. Sol. Cells 95, 1284–1292. http://dx.doi.org/10.1016/j.solmat.2010.08.033.

IEA, 2014. Technology Roadmap: Solar Photovoltaic Energy.

IEC, 2008. IEC 60904-3, Measurement Principles for Terrestrial Photovoltaic (PV) Solar Devices with Reference Spectral Irradiance Data.

IEC, 2008-2. IEC 60751, Industrial Platinum Resistance Thermometers and Platinum Temperature Sensors.

IEC, 1998. IEC 61724, Photovoltaic System Performance Monitoring: Guidelines for Measurement, Data Exchange and Analysis.

IHS, 2013. IHS Cuts Global Solar Inverter Revenue Forecast in Light of Heavy Price Declines [WWW Document]. http://press.ihs.com/press-release/design-supply-chain-media/ihs-cuts-global-solar-inverter-revenue-forecast-light-heavy-. <http://press.ihs.com/press-release/design-supply-chain-media/ihs-cuts-global-solar-inverter-revenue-forecast-light-heavy-> (accessed 05.19.15).

Ishii, T., Takashima, T., Otani, K., 2011. Long-term performance degradation of various kinds of photovoltaic modules under moderate climatic conditions. Prog. Photovoltaics Res. Appl. 19, 170–179. http://dx.doi.org/10.1002/pip.1005.

Jahn, U., Mayer, D., Heidenreich, M., 2000. International Energy Agency PVPS Task 2: Analysis of the operational performance of the IEA Database PV systems. In: 16th European Photovoltaic Solar Energy Conference and Exhibition.

James, T., Goodrich, A., Woodhouse, M., Margolis, R., Ong, S., 2011. Building-integrated photovoltaics (BIPV) in the residential sector: an analysis of installed rooftop system prices. Energy, 50.

Jordan, D.C., Kurtz, S.R., 2013. Photovoltaic degradation rates-an analytical review. Prog. Photovoltaics Res. Appl. 21, 12–29. http://dx.doi.org/10.1002/pip.1182.

Kajari-Schröder, S., Kunze, I., Köntges, M., 2012. Criticality of cracks in PV modules. Energy Procedia 27, 658–663. http://dx.doi.org/10.1016/j.egypro.2012.07.125.

Kalogirou, S.A., 2013. Solar Energy Engineering: Processes and Systems.

Kymakis, E., Kalykakis, S., Papazoglou, T.M., 2009. Performance analysis of a grid connected photovoltaic park on the island of Crete. Energy Convers. Manage. 50, 433–438. http://dx.doi.org/10.1016/j.enconman.2008.12.009.

Li Causi, S., Castello, S., De Lia, F., 2003. ENEA role in the Italian roof-top programme. 3rd World Conference on Photovoltaic Energy Conversion, vol. 3, pp. 2644–2647.

Lo Brano, V., Ciulla, G., Falco, M.Di., 2014. Artificial neural networks to predict the power output of a PV panel. Int. J. Photoenergy 2014.

Lorenzo, E., Zilles, R., Moretón, R., Gómez, T., Martínez de Olcoz, A., 2013. Performance analysis of a 7-kW crystalline silicon generator after 17 years of operation in Madrid. Prog. Photovoltaics Res. Appl. 22, 1273–1279. http://dx.doi.org/10.1002/pip.2379.

Luthander, R., Widén, J., Nilsson, D., Palm, J., 2015. Photovoltaic self-consumption in buildings: a review. Appl. Energy 142, 80–94. http://dx.doi.org/10.1016/j.apenergy.2014.12.028.

Masa-Bote, D., Castillo-Cagigal, M., Matallanas, E., Caamaño-Martín, E., Gutiérrez, A., Monasterio-Huelín, F., Jiménez-Leube, J., 2014. Improving photovoltaics grid integration through short time forecasting and self-consumption. Appl. Energy 125, 103–113. http://dx.doi.org/10.1016/j.apenergy.2014.03.045.

Meyer, E.L., Van Dyk, E.E., Soiling, A.F.S., 2004. Assessing the reliability and degradation of photovoltaic module performance. Parameters 53, 83–92.

Mondol, J.D., Yohanis, Y.G., Norton, B., 2007. The effect of low insolation conditions and inverter oversizing on the long-term performance of a grid-connected photovoltaic system. Prog. Photovoltaics Res. Appl. 15, 353–368. http://dx.doi.org/10.1002/pip.742.

Moretón, R., Lorenzo, E., Leloux, J., Carrillo, J.M., 2014. Dealing in practice with hot-spots. In: 29th European Photovoltaic Solar Energy Conference and Exhibition, September 2014, Amsterdam.

Munoz, M.a., Alonso-García, M.C., Vela, N., Chenlo, F., 2011. Early degradation of silicon PV modules and guaranty conditions. Sol. Energy 85, 2264–2274. http://dx.doi.org/10.1016/j.solener.2011.06.011.

Muñoz-García, M.A., Marin, O., Alonso-García, M.C., Chenlo, F., 2012. Characterization of thin film PV modules under standard test conditions: results of indoor and outdoor measurements and the effects of sunlight exposure. Sol. Energy 86, 3049–3056. http://dx.doi.org/10.1016/j.solener.2012.07.015.

Ndiaye, A., Charki, A., Kobi, A., Kébé, C.M.F., Ndiaye, P.A., Sambou, V., 2013. Degradations of silicon photovoltaic modules: a literature review. Sol. Energy 96, 140–151. http://dx.doi.org/10.1016/j.solener.2013.07.005.

Orioli, A., Di Gangi, A., 2014. Review of the energy and economic parameters involved in the effectiveness of grid-connected PV systems installed in multi-storey buildings. Appl. Energy 113, 955–969. http://dx.doi.org/10.1016/j.apenergy.2013.08.014.

Peng, P., Hu, A., Zheng, W., Su, P., He, D., Oakes, K.D., Fu, A., Han, R., Lee, S.L., Tang, J., Zhou, Y.N., 2012. Microscopy study of snail trail phenomenon on photovoltaic modules. RSC Adv. 2, 11359. http://dx.doi.org/10.1039/c2ra22280a.

Polverini, D., Field, M., Dunlop, E., Zaaiman, W., 2012. Polycrystalline silicon PV modules performance and degradation over 20 years. Prog. Photovoltaics Res. Appl. 21, 1004–1015. http://dx.doi.org/10.1002/pip.2197.

PvXchange, 2015. www.pvxchange.com [WWW Document]. <http://www.pvxchange.com/default.aspx?template_id=1&langTag=de-DE> (accessed 05.19.15).

Quintana, M.A., King, D.L., McMahon, T.J., Osterwald, C.R., 2002. Commonly observed degradation in field-aged photovoltaic modules. In: Conf. Rec. Twenty-Ninth IEEE Photovolt. Spec. Conf. 2002, pp. 1436–1439. http://dx.doi.org/10.1109/PVSC.2002.1190879.

Ransome, S., Funtan, P., 2005. Why hourly averaged measurement data is insufficient to model PV performance accurately. In: 20th Eur. Photovolt. Sol. Energy Conf., pp. 2752–2755.

Realini, A., 2003. Mean Time Before Failure of Photovoltaic Modules, Final Report BBW 99.0579-MTBF Project.

Reinders, A., Van Dijk, V., Wiemken, E., Turkenburg, W.C., 1999. Technical and economic analysis of grid-connected PV systems by means of simulation. Prog. Photovoltaics 7, 71–82.

Sánchez-Friera, P., Piliougine, M., Peláez, J., Carretero, J., Sidrach de Cardona, M., 2011. Analysis of degradation mechanisms of crystalline silicon PV modules after 12 years of operation in Southern Europe. Prog. Photovoltaics Res. Appl. 19, 658–666. http://dx.doi.org/10.1002/pip.1083.

Sharma, V., Chandel, S.S., 2013. Performance and degradation analysis for long term reliability of solar photovoltaic systems: a review. Renew. Sustain. Energy Rev. 27, 753–767. http://dx.doi.org/10.1016/j.rser.2013.07.046.

Sick, F., Erge, T., 2014. Photovoltaics in Buildings: A Design Handbook for Architects and Engineers.

Widén, J., 2014. Improved photovoltaic self-consumption with appliance scheduling in 200 single-family buildings. Appl. Energy 126, 199–212. http://dx.doi.org/10.1016/j.apenergy.2014.04.008.

Zhang, P., Li, W., Li, S., Wang, Y., Xiao, W., 2013. Reliability assessment of photovoltaic power systems: review of current status and future perspectives. Appl. Energy 104, 822–833. http://dx.doi.org/10.1016/j.apenergy.2012.12.010.

Zhou, W., Yang, H., Fang, Z., 2007. A novel model for photovoltaic array performance prediction. Appl. Energy 84, 1187–1198. http://dx.doi.org/10.1016/j.apenergy.2007.04.006.